AJNR

Echo-planar perfusion MR of moyamoya disease.

K Tsuchiya, S Inaoka, Y Mizutani and J Hachiya

AJNR Am J Neuroradiol 1998, 19 (2) 211-216
http://www.ajnr.org/content/19/2/211

AJNR Am J Neuroradiol 19:211–216, February 1998

Echo-Planar Perfusion MR of Moyamoya Disease

Kazuhiro Tsuchiya, Sayuki Inaoka, Yoshiyuki Mizutani, and Junichi Hachiya

PURPOSE: **Our goal was to assess the value of perfusion MR imaging by using a single-shot echo-planar technique to evaluate the hemodynamics of moyamoya disease.**

METHODS: **We performed echo-planar perfusion studies in 19 patients with a 1.5-T unit, using a free-induction-decay echo-planar sequence for 14 examinations and a turbo-gradient-spin-echo echo-planar sequence for five examinations. After a bolus injection of contrast material, 30 consecutive scans were done in 10 sections every 2 seconds. The data were analyzed to yield time-intensity curves for a region of interest set in the territory of the bilateral middle and/or anterior cerebral arteries in all examinations and to produce semiquantitative flow maps of each section, representing the signal decrease due to passage of contrast material in 17 examinations. The semiquantitative flow maps were compared with single-photon emission CT (SPECT) findings in 11 cases.**

RESULTS: **We detected differences between the cerebral hemispheres and/or focal perfusion abnormalities by the time-intensity curves and semiquantitative flow maps in 15 of the 19 examinations and in 11 of the 17 examinations, respectively. Results of one or both these examinations corresponded with the SPECT findings in nine of the 11 examinations.**

CONCLUSION: **Our results indicate that single-shot echo-planar perfusion MR imaging can sensitively depict hemodynamic abnormalities in moyamoya disease.**

In the diagnosis of ischemic cerebrovascular disease, magnetic resonance (MR) imaging can depict lesions readily and accurately. MR angiography is capable of noninvasively delineating the status of the major intracranial arteries. However, it is not possible to obtain adequate information on changes in hemodynamics by these techniques. Such information can be obtained by single-photon emission computed tomography (SPECT) or positron emission tomography (PET), but perfusion MR imaging is another option to examine cerebral blood flow. By using $T2^*$-weighted imaging that is sensitive to magnetic susceptibility, perfusion MR imaging shows signal changes that occur in the brain during the first pass of gadolinium-based contrast material (1–3). For this purpose, gradient-echo sequences have commonly been used. Recently, it has become possible to apply the single-shot echo-planar technique to perfusion MR imaging. As is well known, extremely fast scanning is possible, because this technique acquires sufficient echoes after the application of a single radio-frequency excitation pulse. In the present study, we assessed the value of single-shot echo-planar perfusion MR imaging in the evaluation of hemodynamics in moyamoya disease.

Received June 3, 1997; accepted after revision August 20.

Presented at the annual meeting of the American Society of Neuroradiology, Toronto, Ontario, Canada, May 1997.

From the Department of Radiology, Kyorin University School of Medicine, 6–20–2, Shinkawa, Mitaka, Tokyo 181-8611, Japan. Address reprint requests to Kazuhiro Tsuchiya, MD.

Methods

We performed perfusion MR imaging in 19 patients with moyamoya disease diagnosed by conventional angiography between September 1995 and February 1997. The group consisted of 13 female and six male subjects ranging in age from 9 to 59 years (mean, 24 years).

MR examinations were done with a 1.5-T unit (Magnetom Vision). For 14 examinations, we used a free-induction-decay echo-planar sequence with the following imaging parameters: echo time, 54; scanning time per section, 102 milliseconds; imaging matrix, 128 × 128; and section thickness, 7 mm. For the remaining five examinations, we used a turbo-gradient-spin-echo echo-planar sequence. The imaging parameters were as follows: echo time, 18; scanning time per section, 140 milliseconds; imaging matrix, 128 × 128; and section thickness, 3 mm. For each sequence, we did 30 scans every 2 seconds, with 10 sections in each scan. The 10 sections were set to cover an area from the base of the posterior fossa to the high convexity. A bolus of contrast material (0.1 mmol/kg) was manually injected via the antecubital vein at the start of imaging.

We analyzed the acquired data in three ways. First, time-intensity curves were calculated for two regions of interest (ROIs) of the same size (4 cm^2 or more) in the territory of the middle cerebral artery (MCA) and/or anterior cerebral artery bilaterally (19 examinations). The ROIs were thus placed because moyamoya disease involves the internal carotid artery. The location and size of the ROIs varied case by case based on

Echo-planar perfusion MR imaging findings

Case	Age, y/ Sex	Imaging Sequence	MR Findings	Digital Subtraction Angiography/MR Angiography	Time-Intensity Curves	Flow Maps	Comparison with SPECT
1	26/M	TGSE	Multiple infarcts	R = L	R MCA peak/washout delay and lowered peak	···	···
2	23/F	TGSE	Old putaminal hematoma	R = L	R MCA peak delay	Unremarkable	···
3	21/F	TGSE	Old periventricular hematoma	R > L	R MCA/ACA peak delay	Hypoperfusion in R MCA area	Corresponding findings
4	31/F	TGSE	Unremarkable	R < L	L MCA peak delay, R MCA lowered peak	Unremarkable	Corresponding findings
5	14/M	TGSE	Atrophy, old infarcts	R = L	R MCA peak delay	Multiple hypoperfusion areas	···
6	46/F	FID	Lacunar infarcts	R < L	L ACA peak delay	···	···
7	12/M	FID	Atrophy, old infarcts	R = L	R MCA/ACA peak delay	Hypoperfusion in infarcted areas	Corresponding findings
8	25/F	FID	Unremarkable	R < L	R MCA peak delay and lowered peak	Hypoperfusion in L MCA/PCA area	···
9	18/F	FID	Old hematoma	R < L	R MCA peak delay, R MCA heightened peak	Hypoperfusion in L MCA area	···
10	31/F	FID	Lacunar infarcts	R = L	Unremarkable	Unremarkable	Corresponding findings
11	14/M	FID	Lacunar infarcts	R = L	R MCA peak/washout delay and lowered peak	Multiple hypoperfusion areas	Noncorresponding findings
12	13/F	FID	Old infarcts	R = L	R MCA lowered peak	Hypoperfusion in infarcted areas	···
13	11/M	FID	Old infarcts	R < L	Unremarkable	Hypoperfusion in infarcted areas	Corresponding findings
14	30/F	FID	Lacunar infarcts	R = L	L MCA peak/washout delay	Hypoperfusion in L MCA area	Noncorresponding findings
15	21/M	FID	Lacunar infarcts	R = L	Unremarkable	Unremarkable	Corresponding findings
16	9/F	FID	Unremarkable	R < L	L MCA/ACA heightened peak	Unremarkable	···
17	59/F	FID	Old infarcts	R = L	Unremarkable	Hypoperfusion in infarcted areas	Corresponding findings
18	41/F	FID	Old periventricular hematoma	R < L	L MCA/ACA peak delay	Unremarkable	Corresponding findings
19	10/F	FID	Intraventricular hematoma	R = L	R MCA peak delay, R MCA heightened peak	Hypoperfusion in R MCA area	Corresponding findings

Note.—TGSE indicates turbo-gradient-spin-echo; FID, free-induction decay; MCA, middle cerebral artery; and ACA, anterior cerebral artery.

findings on conventional or MR angiograms. Second, semiquantitative flow maps of each section were created by the software incorporated into the MR unit (17 examinations). These maps were created on the premise that a bolus of gadolinium-based contrast agent produces a decrease in signal intensity of perfused brain tissue on $T2^*$-weighted images. The flow maps showed differences both in the degree of signal decrease due to passage of contrast material and in the time between the start and the peak of the signal. In these maps, the longer the time between the start and the peak of signal decrease and/or the smaller the degree of signal drop, the darker a pixel became. Thus, these maps reflected not only the regional cerebral blood volume but also the difference in arrival time of the contrast material. Therefore, they represented the relative status of the regional cerebral blood flow. Third, the semiquantitative flow maps were compared with axial SPECT scans obtained with ^{123}I-iodoamphetamine (five examinations) or ^{99m}Tc-ethylcysteinate dimer (six examinations), for a total of 11 examinations. We used two SPECT scanners of the same type (GCA-9300A/HG) with a low-energy, super-high-resolution fan-beam collimator with resolution of 8-mm full width at half maximum. The MR and SPECT studies were performed within an interval of 4 weeks.

Results

Differences between the cerebral hemispheres and/or focal perfusion abnormalities were detected with at least one of the three methods of analysis in all except two patients (cases 10 and 15), in whom the time-intensity curves, flow maps, and SPECT scans were unremarkable (Table). In these patients, we believe that, as discussed later, several factors, including the compensation of blood flow due to collateral circulation, were responsible for the perfusion MR imaging findings. Although flow maps of sections near the skull base tended to be distorted by susceptibility artifacts, we could obtain results not degraded by other factors, such as patient motion.

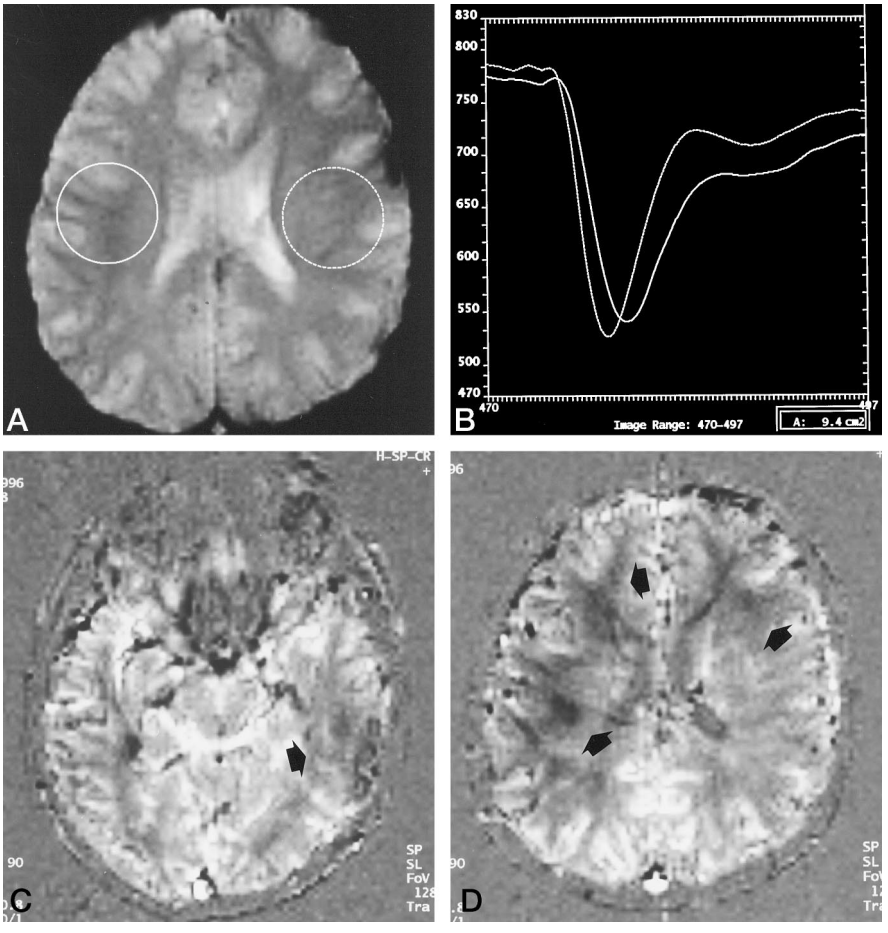

FIG 1. Case 11: 14-year-old boy with moyamoya disease affecting both sides almost equally. The patient had several lacunar infarctions in the bilateral frontal lobes and the right parietal lobe on conventional MR images.

A, Free-induction-decay echo-planar image (echo time, 54; flip angle, 90°; field of view (FOV), 22 × 22 cm; matrix, 128 × 128) shows circular ROIs in the bilateral MCA territories.

B, Time-intensity curves show a delayed peak time and washout as well as a decreased peak height in the right MCA territory (*solid line*) compared with the left MCA territory (*dotted line*).

C and *D*, Flow maps show hypoperfusion in the left temporal, right frontoparietal, and left frontal regions (*arrows*). This abnormality was depicted only on the perfusion study.

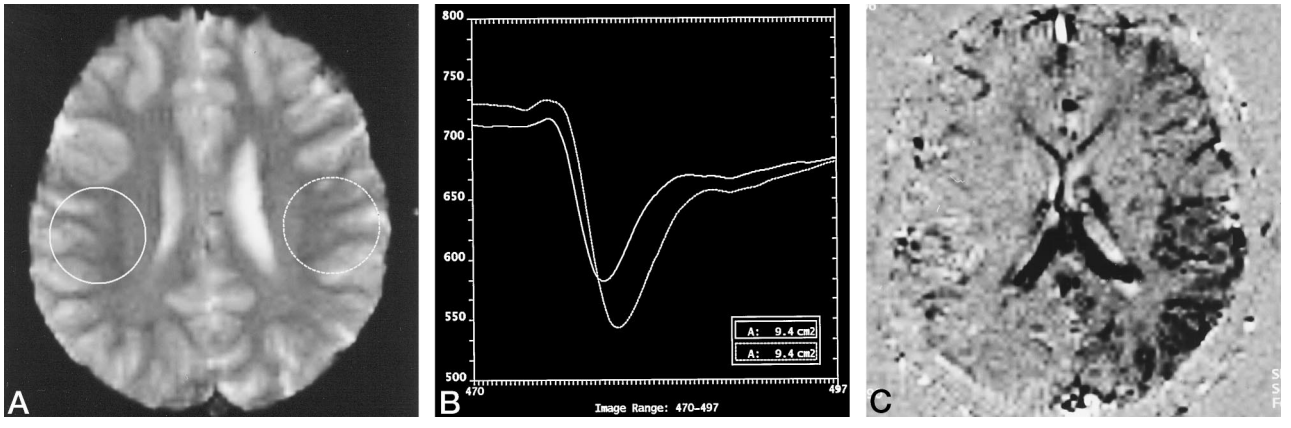

FIG 2. Case 4: 31-year-old woman with moyamoya disease predominantly affecting the left side. MR images showed a small infarction in the right frontal subcortex.

A, Free-induction-decay echo-planar image (echo time, 54; flip angle, 90°; FOV, 22 × 22 cm; matrix, 128 × 128) shows circular ROIs in the bilateral MCA territories.

B, Time-intensity curves show an increased peak height and a delayed peak time in the left MCA territory (*dotted line*) compared with the right MCA territory (*solid line*). The baseline on the right side is lower than that on the left side, because the ROI on the left includes more of the hyperintense cerebrospinal fluid in the sulci than does the one on the right.

C, Flow map shows hypoperfusion in the left MCA and posterior cerebral artery territories, probably reflecting the peak time delay. The hypoperfusion was not seen on conventional MR images, but was suspected at MR angiography.

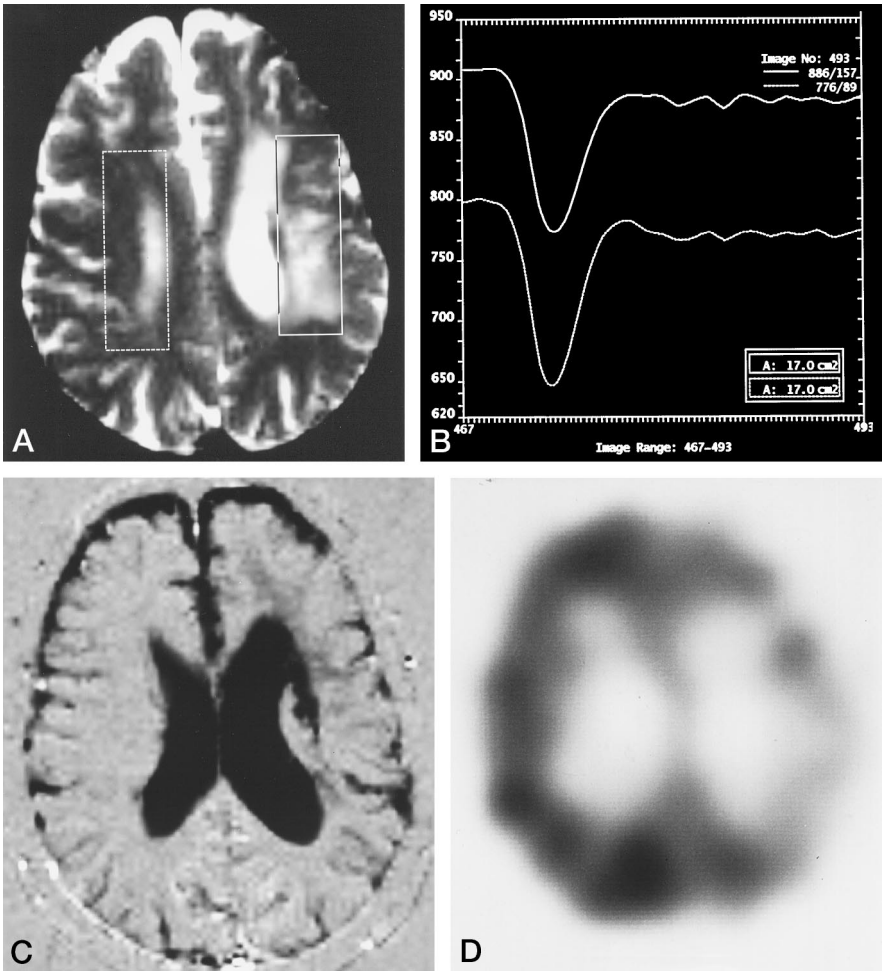

FIG 3. Case 17: 59-year-old woman with moyamoya disease equally affecting both sides. MR images showed a partially hemorrhagic old infarction in the left frontal lobe.

A, Free-induction-decay echo-planar image (echo time, 54; flip angle, 90°; FOV, 22 × 22 cm; matrix, 128 × 128) shows rectangular ROIs in the bilateral MCA territories.

B, Time-intensity curves show a slightly decreased peak height in the left MCA territory (*solid line*) compared with the right MCA territory (*dotted line*).

C, Flow map shows mild hypoperfusion in the left frontoparietal region.

D, SPECT scan obtained with ^{123}I-iodoamphetamine shows corresponding changes. In this patient, the perfusion study revealed an abnormality consistent with the findings on MR and SPECT studies. However, hypoperfusion in the gray matter is more apparent on this SPECT scan than on the flow map.

Time-Intensity Curves (n = 19)

We detected abnormalities in 15 studies (79%). In either of the cerebral hemispheres, the peak was delayed in 13 studies (68%) and washout of contrast material was delayed in three studies (16%) (Fig 1). We noticed decreased signal drop on one side in five studies (26%). In three studies (16%), however, signal drop was increased on the side on which the stenosis was more prominent on conventional or MR angiograms (Fig 2).

Semiquantitative Flow Maps (n = 17)

The flow maps showed focal abnormalities corresponding to infarcted areas on MR images in four studies (24%) (Fig 3); noncorresponding abnormalities were detected in seven studies (41%) (Fig 1). In six studies (35%), the flow maps were normal (Fig 4). Five of these six patients were asymptomatic, and one patient (case 2) had mild hemiparesis.

Comparison of Semiquantitative Flow Maps with SPECT (n = 11)

The flow maps and the SPECT findings corresponded well in nine studies (82%) (Figs 3 and 4), but did not correspond in two studies (18%).

Discussion

Moyamoya disease is a rare cerebrovascular occlusive disorder most often encountered among the Japanese (4–6). It is characterized by progressive occlusion of the supraclinoid portion of the internal carotid artery and the proximal portions of the anterior cerebral artery and the MCA. These occlusive changes are accompanied by the formation of extensive collateral vessels in the basal ganglia and thalamus, together with leptomeningeal and transdural collateral vessels. As a result, cerebral ischemia tends to occur in children, whereas intracranial hemorrhage is more frequent in adults. Although the usefulness of CT, MR imaging, and MR angiography for the diagnosis of moyamoya disease has already been established (7–9), conventional angiography is still necessary for a definitive diagnosis. To evaluate hemodynamic changes in moyamoya disease, SPECT is the method used most widely (10, 11). SPECT findings, especially those of hypoperfusion, generally correlate well with clinical symptoms (10). PET with $H_2{}^{15}O$ or $C^{15}O_2$ is also used at institutions in which it is available (12). The information obtained by these techniques significantly influences assessment of the prognosis and the need to perform bypass surgery.

Currently, perfusion MR imaging is performed us-

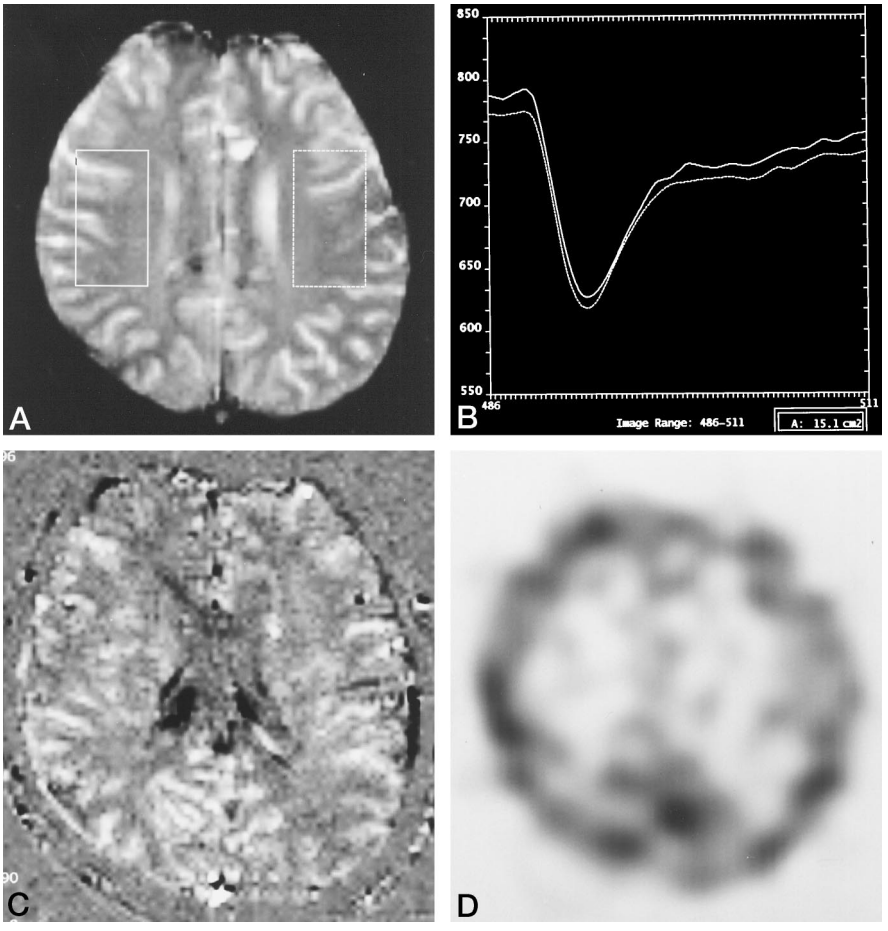

FIG 4. Case 15: 21-year-old man with moyamoya disease affecting both sides equally. Lacunar infarctions were present in the bilateral frontal and parietal lobes.

A, Free-induction-decay echo-planar image (echo time, 54; flip angle, 90°; FOV, 22 × 22 cm; matrix, 128 × 128) shows rectangular ROIs in the bilateral MCA territories.

B, Time-intensity curves are unremarkable.

C, Flow map shows no focal abnormalities, probably because of good collateral flow.

D, SPECT scan obtained with ^{123}I-iodoamphetamine also shows no focal lesions.

ing fast T2*-weighted imaging to detect signal changes that occur during the first pass of contrast material. The value of perfusion MR imaging as well as of diffusion-weighted MR imaging in acute stroke has been described (13, 14). Meanwhile, the efficacy of SPECT and PET in the evaluation of regional cerebral blood flow has been established. However, if perfusion MR imaging can provide comparable information at the same time as standard MR imaging and MR angiography, it would be quite advantageous clinically. Furthermore, perfusion MR imaging is superior to SPECT and PET in the evaluation of blood flow in the white matter. If not postprocessed and displayed properly, the data generated by these techniques cannot demonstrate white matter perfusion well because of the relative hyperperfusion of the gray matter and basal ganglia. Additionally, perfusion MR imaging causes no radiation exposure, which is an advantage over SPECT and PET, because patients with moyamoya disease need repeated examination during a long follow-up period. In the present series, the time-intensity curves revealed a difference between the hemispheres in 79% of the patients. Although moyamoya disease usually involves both hemispheres, its severity is not always symmetric. Presumably, the excellent temporal resolution of single-shot echo-planar sequences allowed us to detect differences between the hemispheres. It is also noteworthy that some patients showed a more marked signal drop on the side on which stenotic change was more prominent on conventional or MR angiograms. We assume that this may be explained by the rich collateral flow in these patients being reflected as seemingly increased perfusion caused by a high sensitivity to magnetic susceptibility. A method of calculating regional blood flow from time-intensity curves obtained by echo-planar perfusion studies has already been proposed (15). Such a quantitative technique would make echo-planar perfusion MR imaging a more valuable tool for patients with various ischemic cerebrovascular disorders, including moyamoya disease. However, setting a proper ROI remains a problem in relation to generating time-intensity curves in moyamoya disease.

Semiquantitative flow maps showed areas of hypoperfusion that either did or did not correspond to infarction in two thirds of our patients. We consider that the multisection capability of echo-planar contributed to the detection of these abnormal foci. Hypoperfusion in the noninfarcted regions thus detected is of clinical importance, because these areas are vulnerable to ischemia. Even the apparently normal flow maps in six (35%) of the 17 examinations may at least partly be attributed to well-developed collateral flow. Thus, the ability of single-shot echo-planar perfusion studies to reveal the whole brain appears to be quite advantageous in moyamoya disease, in which a complicated collateral circulation develops. The flow

map method used in this study is not ideal for visual assessment of perfusion, but quantitative assessment of perfusion may become possible with further developments in software for postprocessing.

The fact that two patients with lacunar infarctions on MR images had normal perfusion studies is somewhat noteworthy. We think well-developed collateral flow was the main cause of the discrepant findings. However, inadequate spatial resolution of flow maps and improperly sized ROIs for the time-intensity curves may also have affected the results.

Echo-planar perfusion MR imaging has several disadvantages. Image degradation by susceptibility artifacts is a problem near the skull base or paranasal sinuses. At present, the spatial resolution is also inadequate. Additionally, although each scan is performed in a very short time, useful data cannot be obtained from patients who do not remain still during the whole imaging examination (about 1 minute).

Conclusions

Our results indicate that single-shot echo-planar perfusion MR imaging can sensitively detect abnormalities of hemodynamics in patients with moyamoya disease. We think that the multisection capability and excellent temporal resolution of this technique are most advantageous. In this study, it was unfortunate that only a limited number of examinations could be compared with SPECT. Additionally, a more sophisticated method of data analysis may be required. Nevertheless, our results suggest that echo-planar perfusion MR imaging has the potential to become an effective diagnostic tool comparable to SPECT or PET in evaluating moyamoya disease.

Acknowledgments

We gratefully acknowledge Takahito Miyazawa and Shigeru Kosuda, National Defense Medical College, Tokorozawa, Saitama, Japan, for their support in performing this study.

References

1. Belliveau JW, Rosen BR, Kantor HL, et al. **Functional cerebral imaging by susceptibility-contrast NMR.** *Magn Reson Med* 1990;14: 538–546
2. Edelman RR, Mattle HP, Atkins DJ, et al. **Cerebral blood flow: assessment with dynamic contrast-enhanced T2*-weighted MR imaging at 1.5T.** *Radiology* 1990;176:211–220
3. Villringer A, Rosen RB, Belliveau JW, et al. **Dynamic imaging with lanthanide chelates in normal brain: contrast due to magnetic susceptibility effects.** *Magn Reson Med* 1988;6:164–174
4. Kudo T. **Spontaneous occlusion of the circle of Willis.** *Neurology* 1968;18:485–496
5. Suzuki J, Takaku A. **Cerebrovascular "moyamoya" disease: disease showing abnormal net-like vessels in base of the brain.** *Arch Neurol* 1969;20:288–299
6. Suzuki J, Kodama N. **Moyamoya disease: a review.** *Stroke* 1983;14: 104–109
7. Takahashi M, Miyauchi T, Kowada M. **Computed tomography of moyamoya disease: demonstration of occluded arteries and collateral vessels as important diagnostic signs.** *Radiology* 1980;134:671–676
8. Fujisawa I, Asato R, Nishimura K, et al. **Moyamoya disease: MR imaging.** *Radiology* 1987;164:103–105
9. Yamada I, Matsushima Y, Suzuki S. **Moyamoya disease: diagnosis with three-dimensional time-of-flight MR angiography**. *Radiology* 1992;184:773–778
10. Mountz JM, Foster NL, Ackermann RJ, Bluemlein L, Petry NA, Kuhl DE. **SPECT imaging of moyamoya disease using 99mTc-HM-PAO: comparison with computed tomography**. *J Comput Assist Tomogr* 1988;12:247–250
11. Hoshi H, Ohnishi T, Jinnouchi S, et al. **Cerebral blood flow study in patients with moyamoya disease evaluated by IMP SPECT**. *J Nucl Med* 1994;35:44–50
12. Kuwabara Y. **Evaluation of regional cerebral circulation and metabolism in moyamoya disease using positron emission computed tomography.** *Jpn J Nucl Med* 1986;23:1381–1402
13. Warach S, Li W, Ronthal M, Edelman RR. **Acute cerebral ischemia: evaluation with dynamic contrast-enhanced MR imaging and MR angiography.** *Radiology* 1992;182:41–47
14. Warach S, Dashe JF, Edelman RR. **Clinical outcome in ischemic stroke predicted by early diffusion-weighted and perfusion magnetic resonance imaging: a preliminary analysis.** *J Cereb Blood Flow Metab* 1996;16:53–59
15. Aronen HJ, Gazit IE, Louis DN, et al. **Cerebral blood volume maps of gliomas: comparison with tumor grade and histologic findings.** *Radiology* 1994;191:41–51